

# $\eta$ and $\eta'$ masses and decay constants from lattice QCD with $N_f = 2 + 1 + 1$ quark flavours

---

**K. Ottnad<sup>\*†</sup>, C. Urbach**

*HISKP (Theory), University of Bonn, Nussallee 14-16, Bonn, Germany*

*E-mail: urbach@hiskp.uni-bonn.de*

**Chris Michael**

*Theoretical Physics Division, Department of Mathematical Sciences*

*The University of Liverpool, Liverpool, L69 3BX, UK*

*E-mail: c.michael@liv.ac.uk*

**for the European Twisted Mass collaboration**

We investigate the masses and decay constants of  $\eta$  and  $\eta'$  mesons using the Wilson twisted mass formulation with  $N_f = 2 + 1 + 1$  dynamical quark flavours based on gauge configurations of ETMC. We show how to efficiently subtract excited state contributions to the relevant correlation functions and estimate in particular the  $\eta'$  mass with improved precision. After investigating the strange quark mass dependence and the continuum and chiral extrapolations, we present our results for masses and mixing angle(s) at the physical point. Using chiral perturbation theory we also extract the decay constants  $f_l$  and  $f_s$ , and use them to estimate the decay widths of  $\eta, \eta' \rightarrow \gamma\gamma$  and the transition form factor in the limit of large momentum transfer.

*31st International Symposium on Lattice Field Theory - LATTICE 2013*

*July 29 - August 3, 2013*

*Mainz, Germany*

---

<sup>\*</sup>Speaker.

<sup>†</sup>current affiliation: University of Cyprus, Nicosia, Cyprus

ensemble	$\beta$	$a\mu_l$	$a\mu_\sigma$	$a\mu_\delta$	$L/a$	$N_{\text{conf}}$	$N_s$	$N_b$
A30.32	1.90	0.0030	0.150	0.190	32	1367	24	5
A40.24	1.90	0.0040	0.150	0.190	24	2630	32	10
A40.32	1.90	0.0040	0.150	0.190	32	863	24	4
A60.24	1.90	0.0060	0.150	0.190	24	1251	32	5
A80.24	1.90	0.0080	0.150	0.190	24	2449	32	10
A100.24	1.90	0.0100	0.150	0.190	24	2493	32	10
A80.24 <sub>s</sub>	1.90	0.0080	0.150	0.197	24	2517	32	10
A100.24 <sub>s</sub>	1.90	0.0100	0.150	0.197	24	2312	32	10
B25.32	1.95	0.0025	0.135	0.170	32	1484	24	5
B35.32	1.95	0.0035	0.135	0.170	32	1251	24	5
B55.32	1.95	0.0055	0.135	0.170	32	1545	24	5
B75.32	1.95	0.0075	0.135	0.170	32	922	24	4
B85.24	1.95	0.0085	0.135	0.170	24	573	32	2
D15.48	2.10	0.0015	0.120	0.1385	48	1045	24	10
D30.48	2.10	0.0030	0.120	0.1385	48	469	24	3
D45.32 <sub>sc</sub>	2.10	0.0045	0.0937	0.1077	32	1887	24	10

**Table 1:** The ensembles used in this investigation. For the labelling we employ the notation of ref. [5]. Additionally, we give the number of configurations  $N_{\text{conf}}$ , the number of stochastic samples  $N_s$  for all ensembles and the bootstrap block length  $N_b$ . The D30.48 ensemble was not yet included in Ref. [2].

## 1. Introduction

$\eta$  and  $\eta'$  mesons are very interesting from a theoretical point of view, because they are directly related to the  $U_A(1)$  anomaly and topology in QCD. They are challenging to investigate in lattice QCD due to significant disconnected contributions. In a series of papers and proceeding contributions we have presented results for the corresponding meson masses and the mixing angle(s) [1, 2, 3, 4] using  $N_f = 2 + 1 + 1$  Wilson twisted mass fermions. In this proceeding we extend our analysis towards  $\eta$  and  $\eta'$  decay constants using pseudoscalar matrix elements and chiral perturbation theory.

The results we present are based on gauge configurations provided by the European Twisted Mass Collaboration (ETMC) and correspond to three values of the lattice spacing,  $a = 0.061$  fm,  $a = 0.078$  fm and  $a = 0.086$  fm. The pion masses range from 230 to 500 MeV [5, 6]. A list of the investigated ensembles is given in Table 1. For setting the scale we use throughout this proceeding contribution the Sommer parameter  $r_0 = 0.45(2)$  fm [6].

We use the Wilson twisted mass formulation of lattice QCD [7, 8] with the main advantage of automatic  $\mathcal{O}(a)$  improvement at maximal twist [9] and the disadvantage that parity and flavour symmetry are both broken at finite values of the lattice spacing. The latter was shown to affect mainly the value of the neutral pion mass [10, 11, 12]. Furthermore, for the non-degenerate quark doublet this introduces mixing between charm and strange quarks. For details on the lattice action we refer to Ref. [5].

## 2. Pseudoscalar flavour-singlet mesons

We compute the Euclidean correlation functions

$$\mathcal{C}(t)_{qq'} = \langle \mathcal{O}_q(t'+t) \mathcal{O}_{q'}(t') \rangle, \quad q, q' \in l, s, c, \quad (2.1)$$

with operators  $\mathcal{O}_l = (\bar{u}i\gamma_5 u + \bar{d}i\gamma_5 d)/\sqrt{2}$ ,  $\mathcal{O}_s = \bar{s}i\gamma_5 s$  and  $\mathcal{O}_c = \bar{c}i\gamma_5 c$ . We enlarge our correlator matrix  $\mathcal{C}$  by including also fuzzed operators. Note that in twisted mass lattice QCD there are several steps required to reach these correlation functions, as explained in detail in Ref. [2]. We estimate the disconnected contributions to the correlation functions Eq. 2.1 using Gaussian volume sources and the connected contributions [13] using the one-end trick. For the light disconnected contributions a powerful noise reduction technique is available [14, 2]. For the strange and charm disconnected loops, we use the hopping parameter noise reduction technique [13].

We solve the generalised eigenvalue problem (GEVP) [15, 16, 17]

$$\mathcal{C}(t)\eta^{(n)}(t, t_0) = \lambda^{(n)}(t, t_0)\mathcal{C}(t_0)\eta^{(n)}(t, t_0) \quad (2.2)$$

for eigenvalues  $\lambda^{(n)}(t, t_0)$  and eigenvectors  $\eta^{(n)}$ .  $n$  labels the states  $\eta, \eta', \dots$  contributing. Masses of these states can be determined from the exponential fall-off of  $\lambda^{(n)}(t, t_0)$  at large  $t$ . The pseudoscalar matrix elements  $A_{q,n} \equiv \langle n | \mathcal{O}_q | 0 \rangle$  with  $q \in l, s, c$  and  $n \in \eta, \eta', \dots$  can be extracted from the eigenvectors [17]. It turns out that the charm quark contributions to  $\eta, \eta'$  are negligible and, thus, we drop the  $c$  quark in what follows.

### Decay Constants and Mixing

In general, decay constants are defined for any pseudoscalar meson  $P$  from axial vector matrix elements

$$\langle 0 | A_\mu^a | P(p) \rangle = i f_P^a p_\mu, \quad (2.3)$$

which leads to

$$\langle 0 | \partial^\mu A_\mu^a | P(0) \rangle = f_P^a M_P^2, \quad (2.4)$$

for projection to zero momentum. Assuming that  $\eta$  and  $\eta'$  are not flavour eigenstates, each of them exhibits a coupling to the singlet and octet axial vector current  $A_\mu^0$  and  $A_\mu^8$ , respectively. Therefore, one ends up with four independent decay constants for the  $\eta, \eta'$ -system, which are commonly parametrised in terms of two decay constants  $f_0, f_8$  and two mixing angles  $\theta_0, \theta_8$

$$\begin{pmatrix} f_\eta^8 & f_\eta^0 \\ f_{\eta'}^8 & f_{\eta'}^0 \end{pmatrix} = \begin{pmatrix} f_8 \cos \theta_8 & -f_0 \sin \theta_0 \\ f_8 \sin \theta_8 & f_0 \cos \theta_0 \end{pmatrix} \equiv \Xi(\theta_8, \theta_0) \text{diag}(f_8, f_0). \quad (2.5)$$

The singlet decay constant  $f_0$  needs renormalisation, determined by the anomalous dimension of the axial singlet current [18]. The dependence on the scale is  $\mathcal{O}(1/N_C)$  and can, therefore, be dropped in the following discussion. For a detailed discussion see Refs. [19, 20].

On the lattice it is more convenient to work in the quark flavour basis, with the axial vector currents  $A_\mu^0$  and  $A_\mu^8$  replaced by the combinations

$$A_\mu^l = \frac{2}{\sqrt{3}} A_\mu^0 + \sqrt{\frac{2}{3}} A_\mu^8 = \frac{1}{\sqrt{2}} (\bar{u}\gamma_\mu\gamma_5 u + \bar{d}\gamma_\mu\gamma_5 d), \quad (2.6)$$

$$A_\mu^s = \sqrt{\frac{2}{3}} A_\mu^0 - \frac{2}{\sqrt{3}} A_\mu^8 = \bar{s}\gamma_\mu\gamma_5 s, \quad (2.7)$$

in which the light quarks and the strange quark contributions are disentangled. In exact analogy to the singlet-octet basis this basis again allows for a parametrisation in terms of two decay constants and two mixing angles

$$\begin{pmatrix} f_\eta^l & f_\eta^s \\ f_{\eta'}^l & f_{\eta'}^s \end{pmatrix} = \Xi(\phi_l, \phi_s) \text{diag}(f_l, f_s), \quad (2.8)$$

where the mixing matrix  $\Xi$  has the same form as the one defined in Eq. 2.5. In this basis it is also expected that we have [21, 19, 20, 22, 23]

$$\left| \frac{\phi_l - \phi_s}{\phi_l + \phi_s} \right| \ll 1. \quad (2.9)$$

motivating a simplified mixing scheme in the quark flavour basis with only one angle  $\phi$

$$\begin{pmatrix} f_\eta^l & f_\eta^s \\ f_{\eta'}^l & f_{\eta'}^s \end{pmatrix} = \Xi(\phi) \text{diag}(f_l, f_s) + \mathcal{O}(\Lambda_1), \quad (2.10)$$

where  $\Xi(\phi) \equiv \Xi(\phi, \phi)$  and  $\Lambda_1$  parametrises residual OZI violating terms. The mixing angle  $\phi$  is related to the double ratio of amplitudes

$$\tan^2(\phi) = -\frac{f_{\eta'}^l f_\eta^s}{f_\eta^l f_{\eta'}^s}. \quad (2.11)$$

Axial vector current matrix elements turn out to be difficult to measure in actual simulations due to noise. This is why it is most convenient to consider pseudoscalar currents in the quark flavour basis in analogy to Eqs. (2.6),(2.7).

$$P^l = \frac{1}{\sqrt{2}} (\bar{u}\gamma_5 u + \bar{d}\gamma_5 d), \quad (2.12)$$

$$P^s = \bar{s}i\gamma_5 s, \quad (2.13)$$

such that the matrix elements for pseudoscalar mesons P are given by

$$h_P^i = 2m_i \langle 0 | P^i | P \rangle, \quad (2.14)$$

which are free from renormalisation. Making use of  $\chi$ PT and dropping subleading terms leads to the following expression [24]

$$\begin{pmatrix} h_\eta^l & h_\eta^s \\ h_{\eta'}^l & h_{\eta'}^s \end{pmatrix} = \Xi(\phi) \text{diag}(M_\pi^2 f_l, (2M_K^2 - M_\pi^2) f_s). \quad (2.15)$$

This expression allows access to the decay constants  $f_s$  and  $f_l$  from pseudoscalar matrix elements under the assumption that  $\chi$ PT can be applied. In terms of pseudoscalar matrix elements the mixing angle  $\phi$  is obtained as

$$\tan^2(\phi) = -\frac{h_{\eta'}^l h_\eta^s}{h_\eta^l h_{\eta'}^s}, \quad (2.16)$$

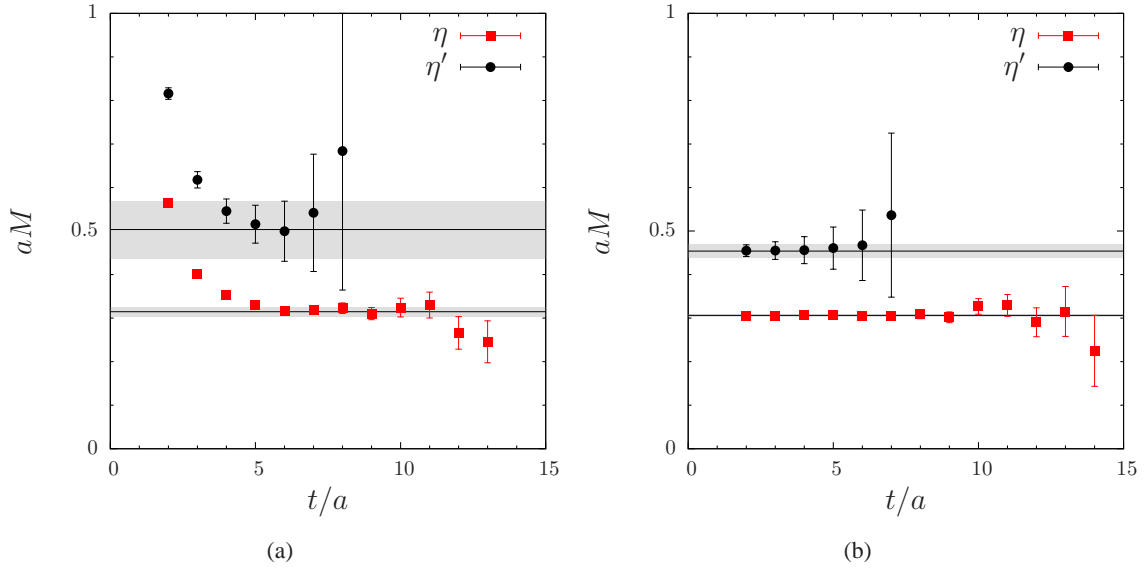


**Figure 1:** (a) Effective masses in lattice units determined from solving the GEVP for a  $6 \times 6$  matrix with  $t_0/a = 1$  for ensemble A100. (b) the same, but after removal of excited states in the connected contributions.

where actually quark masses and renormalisation constants drop out in the ratio. Expanding again to two angles,  $\phi_l$  and  $\phi_s$  are written as

$$\tan(\phi_l) = \frac{h_{\eta'}^l}{h_{\eta}^l}, \quad \tan(\phi_s) = -\frac{h_{\eta}^s}{h_{\eta'}^s}. \quad (2.17)$$

Finally we remark that in order to compute the matrix elements  $h_p^i$  in Wilson twisted mass lattice QCD the ratio of renormalisation constants  $Z_P/Z_S$  is required [2] which we took from Ref. [25].

### 3. Excited State Removal

The result of solving the GEVP for a  $6 \times 6$  matrix for ensemble A100 including fuzzed operators is shown as effective masses in the left panel of figure 1. It is visible that the ground state, the  $\eta$  meson, can be extracted with good precision, while for the  $\eta'$  meson it is unclear that a plateau is reached before the signal is lost in noise.

However, there is a possibility to obtain a significant improvement for the extraction of  $\eta'$  mass (and further observables) using a powerful method to separate ground and excited states, which has first been proposed in [26] and that has already been successfully employed for the case of the  $\eta_2$  for two dynamical quark flavours in [14]. In the following we will describe this method and apply it to our data.

The method is based on the assumption that the quark disconnected diagrams give a sizeable contribution only to the  $\eta$  and  $\eta'$  state, but are negligible for any heavier state with the same quantum numbers. Considering the fluctuations of the topological charge which are expected to give a dominant contribution to the mass of the  $\eta'$ , this assumption would be valid if these fluctuation mainly couple to the  $\eta$  and  $\eta'$  states. Still, the validity of this assumption needs to be carefully checked from our data and may introduce systematic uncertainties.

Since the quark connected contributions exhibit a constant signal-to-noise ratio, it is in principle possible to determine the respective ground states at sufficiently large  $t/a$  with high statistical accuracy and without any significant contamination from higher states. After fitting the respective ground states of the connected correlators, we can use it to subtract the excited state contributions such that the full connected correlators are replaced by correlators that contain only the ground state. Note that for sufficiently large  $t/a$  this reproduces the original ground state by construction.

Now, if the aforementioned assumption holds, i.e. the disconnected diagrams are relevant only to the two lowest states  $\eta$ ,  $\eta'$  one should obtain a plateau in the effective mass at very low values of  $t/a$  after solving the GEVP. The result of the procedure is shown in the right panel of figure 1. Indeed, one observes a plateau for both states starting basically at the lowest possible value of  $t/a$ . Furthermore, a comparison with the effective masses from the standard  $6 \times 6$  matrix in the left panel of figure 1 reveals that the plateau values agree very well within their respective errors. Most importantly, the data in the right panel allows for a much better accuracy in the determination of both masses as the point errors are much smaller at such low values of  $t/a$ . Therefore, we will use this method for all the results presented in this proceeding contribution.

However, we remark that in the twisted mass formulation with the non-degenerate doublet this procedure is in practice restricted to the connected correlation functions corresponding to physical light and strange quarks. This is due to the violation of flavour symmetry in the heavy sector of the twisted mass formulation, implying that the four connected contributions in the heavy sector will all yield the same ground state. This ground state corresponds to an artificial particle, i.e. a connected-only, neutral pion-like particle made out of strange quarks. Therefore, we will restrict ourselves in the following discussion to the analysis of a  $2 \times 2$  correlation function matrix corresponding to (local) physical operators made of light and strange quarks.

#### 4. $\eta$ and $\eta'$ Masses and Extrapolations

We determine the masses using the excited state removal method described in the previous section for all ensembles listed in table 1 and determine  $aM_\eta$  and  $aM_{\eta'}$ . It turns out that in  $aM_\eta$  we see a strange quark mass dependence that we can resolve well within our statistical errors. As the physical values of the strange quark masses vary by about 10% in between the different lattice spacing values, we have to correct for this. This is described in detail in Ref. [2]. Here we will repeat the procedure only shortly: we use the ensembles A80 and A80s (A100 and A100s), which differ in the bare strange quark mass value, to estimate  $D_\eta = dM_\eta^2/dM_K^2$ . Next we correct all  $aM_\eta$  values to correspond to a line of  $M_K[M_{PS}^2]$  values which reproduces the physical kaon mass at  $M_{PS} = M_{\pi^0}^{\text{phys}}$ . These corrected values we denote with  $\bar{M}_\eta$ . Note that for this procedure we ignore any dependence of  $D_\eta$  on the quark masses and the lattice spacing. For the  $\eta'$  mass we do not resolve quark mass or lattice spacing dependence within our errors, so we do not attempt to correct for those.

The results for  $\bar{M}_\eta$  and  $M_{\eta'}$  are summarised in figure 2, where we show  $r_0\bar{M}_\eta$  as filled and  $M_{\eta'}$  as open symbols, respectively, both as functions of  $(r_0M_{PS})^2$ . For both mesons the data fall within errors on a single line such that in both cases we model the data for  $(r_0M)^2$  as constant plus a linear term in  $(r_0M_{PS})^2$ . The corresponding best fit to the data and its error band is shown as lines with shaded bands. The error band for  $M_\eta$  is mainly due to the error of  $D_\eta$ .

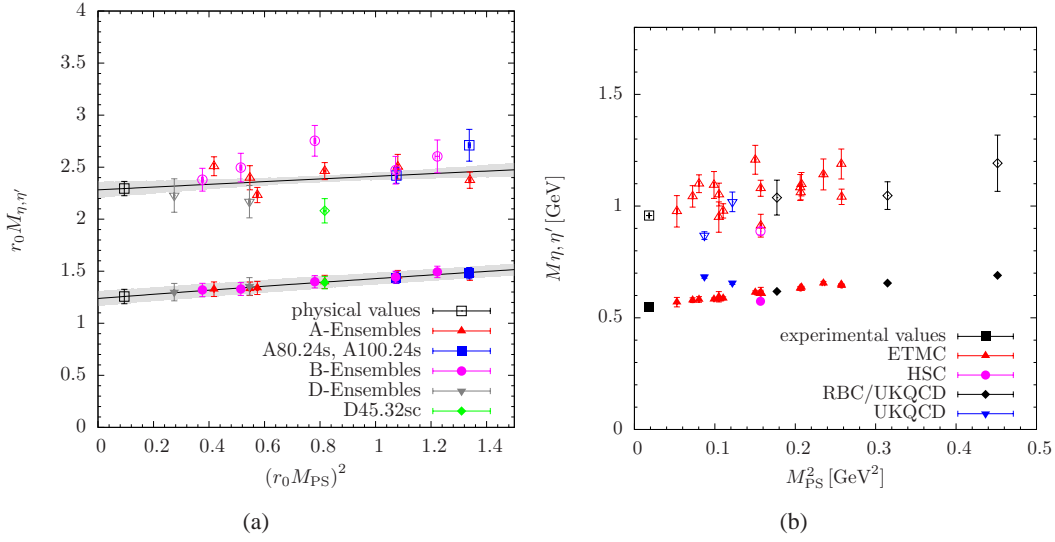


**Figure 2:** (a) Our results for  $r_0 \bar{M}_\eta$  (filled symbols) (corrected for the mismatch in  $r_0 M_K$ ) and  $r_0 M_{\eta'}$  (open symbols). The fitted curves are linear functions in  $(r_0 M_{PS})^2$  as discussed in the text. (b) The same data as in (a), but in physical units and including results from other lattice computations.

After extrapolating to the physical point and converting to physical units we obtain

$$M_\eta(M_\pi) = 551(11)_{\text{stat}}(6)_{\text{sys}} \text{ MeV}, \quad (4.1)$$

where the systematic error has been estimated from fitting to the data at each value of the lattice spacing separately. Note that the value for the physical  $\eta$  mass is in very good agreement with the experimental value  $M_\eta^{\text{exp}} = 547.85(2) \text{ MeV}$  [27]. In addition, for the SU(2) chiral limit we find  $r_0 \hat{M}_\eta^{\text{SU}(2)} = 1.24(7)_{\text{stat}}(2)_{\text{sys}}$ , which yields

$$\hat{M}_\eta^{\text{SU}(2)} = 543(11)_{\text{stat}}(7)_{\text{sys}} \text{ MeV}. \quad (4.2)$$

We may extrapolate further quantities in order to check the validity of our correction procedure for mistuned values of the strange quark mass. First, we consider the GMO ratio determined directly from the data and perform an extrapolation in  $(r_0 M_{PS})^2$ . However, it turns out that taking the uncorrected values of  $M_\eta$  the extrapolation misses the experimental value  $(3M_\eta^2/(4M_K^2 - M_\pi^2))^{\text{exp}} = 0.925$  considering only the statistical error by more than  $2\sigma$ , i.e. we obtain  $(3M_\eta^2/(4M_K^2 - M_\pi^2))_{M_\pi} = 0.963(15)_{\text{stat}}(35)_{\text{sys}}$ . This may be seen as a hint that the significantly increased statistical precision of the improved analysis strategy allows to resolve a residual strange quark mass dependence which is not cancelled in the ratio. This was not possible with the statistical accuracy we could obtain in Ref. [2]. Note that compared to the direct extrapolation the statistical precision is even further enhanced for the case of dimensionless ratios because the physical value of  $r_0$  is only required for fixing the physical point, but not for the conversion to physical units. Considering only the *B* ensembles for which the value of the strange quark mass is close to physical yields  $(3M_\eta^2/(4M_K^2 - M_\pi^2))_{M_\pi}^B = 0.928(27)_{\text{stat}}$ , indicating that the systematic error is mainly caused by such a residual effect. Indeed, using the corrected values  $\bar{M}_\eta$  and the corresponding values of the kaon mass to calculate the GMO ratio the extrapolation gives  $(3M_\eta^2/(4M_K^2 - M_\pi^2))_{M_\pi} =$

$0.946(26)_{\text{stat}}(22)_{\text{sys}}$ , which agrees nicely with the experimental value and exhibits a smaller systematic error compared to the result obtained from using the uncorrected values of  $M_\eta$ . For the physical value of the  $\eta$  mass we obtain

$$M_\eta = 554(8)_{\text{stat}}(7)_{\text{sys}} \text{ MeV}, \quad (4.3)$$

in agreement with the result from the direct extrapolation and the experimental value.

A similar picture arises from the light quark mass extrapolation of the ratio  $M_\eta/M_K$ . Using the uncorrected values of  $M_\eta$  which yields  $(M_\eta/M_K)_{M_\pi} = 1.117(8)_{\text{stat}}(23)_{\text{sys}}$ , missing the experimental value  $(M_\eta/M_K)^{\text{exp}} = 1.100$  again by roughly  $2\sigma$  if taking only the statistical error into account. Like for the case of the GMO ratio taking only the *B* ensembles into account gives nice agreement with the experimental value, i.e.  $(M_\eta/M_K)_{M_\pi}^B = 1.117(8)_{\text{stat}}$ , whereas *A* and *D* ensembles give significantly larger values. Therefore, we have also repeated the extrapolation using the corrected values  $\bar{M}_\eta$  and the corresponding kaon masses. Within the statistical errors one again obtains excellent agreement with experiment, i.e.  $(M_\eta/M_K)_{M_\pi} = 1.099(16)_{\text{stat}}(19)_{\text{sys}}$ , which results in

$$M_\eta = 0.547(8)_{\text{stat}}(9)_{\text{sys}} \text{ MeV}, \quad (4.4)$$

compatible with the results from direct and GMO ratio extrapolations.

In order to obtain our final result for the physical mass of the  $\eta$  we take the weighted average from the three previously discussed methods used for the extrapolation in the light quark mass. Accounting for any correlations, this yields

$$M_\eta = 551(8)_{\text{stat}}(6)_{\text{sys}}. \quad (4.5)$$

which is in excellent agreement with experiment and exhibits substantially smaller errors compared to Ref. [2].

For the  $\eta'$  we obtain

$$M_{\eta'} = 1006(54)_{\text{stat}}(38)_{\text{sys}}(+61)_{\text{ex}}, \quad (4.6)$$

from a linear extrapolation in  $(r_0 M_{\text{PS}})^2$  of all the (uncorrected) data. In order to quantify a possible error introduced by the excited state removal in the connected contributions, we quote the difference between the extrapolations with and without excited state removal as an additional systematic error. Again, the standard systematic error has been determined from fits to the data at single values of the lattice spacing and it is interesting to note that it actually turns out to be the smallest of the three errors. Within the larger errors this result is again in very good agreement with experiment, confirming that QCD indeed accounts for the significantly larger mass of the  $\eta'$  that is observed experimentally.

In the right panel of figure 2 we show a compilation of our results for  $\eta$  and  $\eta'$  masses together with results available in the literature for  $N_f = 2 + 1$  flavour lattice QCD. For  $M_\eta$  we show the values corrected for the mismatch in  $M_K$ . We remark that in [28]  $\eta$  and  $\eta'$  meson masses have been computed using  $N_f = 2 + 1$  flavours of overlap quarks at one value of the lattice spacing and large values of the pion mass, however, in this reference not enough details are given to be included in our comparison figure 2. The results in [29] have been obtained using  $N_f = 2 + 1$  flavours of domain wall fermions and again for a single value of the lattice spacing  $a \approx 0.1 \text{ fm}$  but

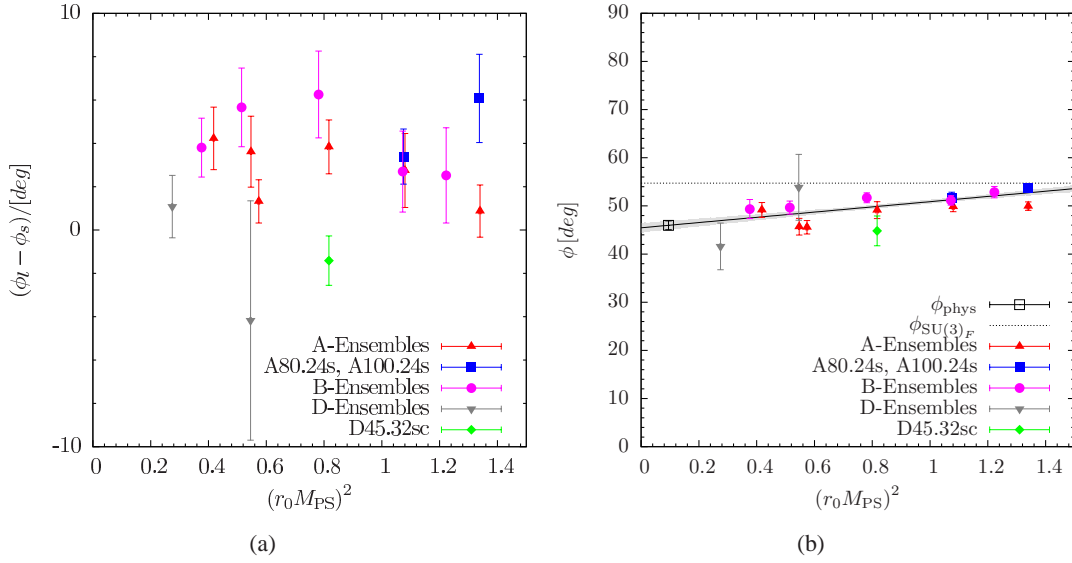


**Figure 3:** (a) the difference  $\phi_l - \phi_s$  in degrees and (b)  $\phi$  as functions of  $(r_0 M_{PS})^2$ .

for three values of the pion mass in a range from  $\sim 400\text{MeV}$  to  $\sim 700\text{MeV}$ . The corresponding data points in figure 2 are labelled “RBC/UK QCD”. Another single data point is added from [30] by the Hadron Spectrum Collaboration (HSC) for which Wilson fermions have been employed. Again, it was not possible to include more recent results by the HSC [31] due to the lack of explicit numerical values in this reference for the relevant masses. Finally, in [32] data from staggered fermions are presented for two different values of the lattice spacing with each of them also at a different value of the pion mass. In figure 2 the corresponding data points are labelled “UKQCD”. The figure suggests an overall agreement between all collaborations.

### 5. $\eta, \eta'$ -mixing Angles

The mixing angles  $\phi_l$  and  $\phi_s$  can be extracted using Eq. 2.17 with a mixing model based on the pseudoscalar matrix elements  $h_p^q$ . In the left panel of figure 3 we show  $\phi_l - \phi_s$  in degrees as a function of  $(r_0 M_{PS})^2$ . One observes that this quantity is consistent with zero within errors. Also an extrapolation to the physical point yields  $3(1)_{\text{stat}}(3)_{\text{sys}}^\circ$ , where the systematic error is estimated from the maximal difference compared to extrapolating the data sets for the three different lattice spacings separately.

In the right panel of figure 3 we show the average angle  $\phi$  (Eq. 2.16) in degrees as a function of  $(r_0 M_{PS})^2$ , with smaller statistical errors than  $\phi_l$  and  $\phi_s$  separately, because of correlation in the matrix elements. Our precision is not sufficient to resolve any residual lattice spacing or strange quark mass dependence. Hence, we extrapolate linearly in  $(r_0 M_{PS})^2$  and obtain

$$\phi = 46(1)_{\text{stat}}(3)_{\text{sys}}^\circ, \tag{5.1}$$

where the first error is statistical and the second systematic from fitting the three values of the lattice spacing separately.

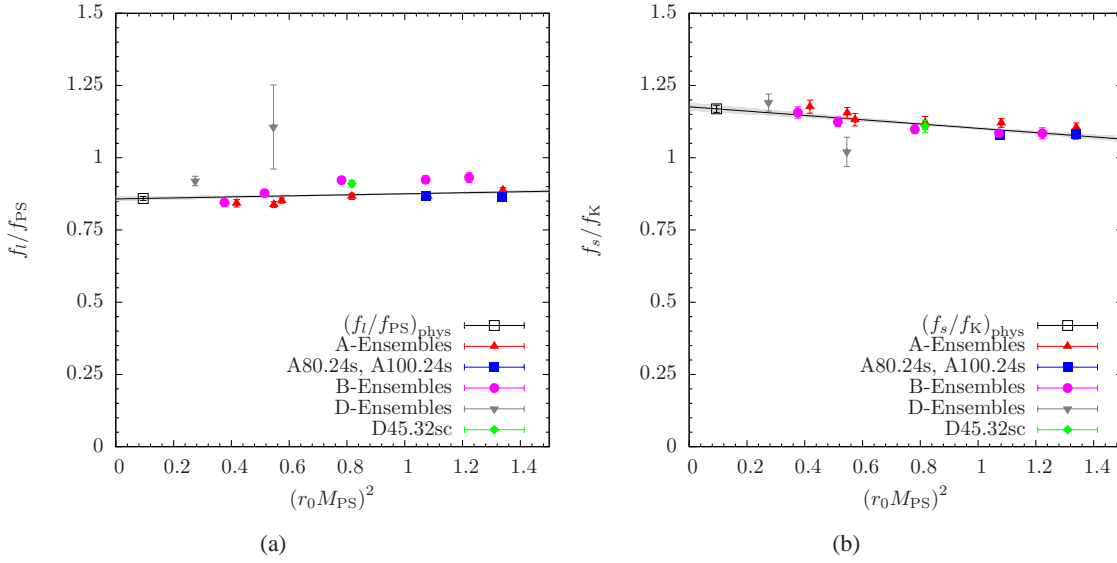


**Figure 4:** (a)  $f_l/f_{PS}$  and (b)  $f_l/f_K$  as functions of  $(r_0 M_{PS})^2$ .

Besides the mixing angle  $\phi$ , we consider the angles  $\phi_l$ ,  $\phi_s$  which are relevant to cross-check the assumptions entering our mixing scheme. Again, we have performed linear fits in  $(r_0 M_{PS})^2$  and obtain at the physical value of the pion mass

$$\phi_l = 48(1)_{\text{stat}}(4)_{\text{sys}}^\circ, \quad \phi_s = 44(1)_{\text{stat}}(3)_{\text{sys}}^\circ, \quad (5.2)$$

where the systematic uncertainties have been determined in the same way as for the angle  $\phi$  itself. The results are compatible within errors. Notably, for  $\phi_s$  there is very good agreement for the results within each of the two set (A80.24, A80.24s) and (A100.24, A100.24s), indicating that the influence of the strange quark is smaller for this quantity and in general more of the data points lie within the error band of the linear fit.

## 6. Decay Constants

The application of the excited state removal method discussed in the previous section allows to extract the decay constants  $f_l$  and  $f_s$  to a rather high statistical precision by means of the pseudoscalar matrix elements  $h_p^i$  and using Eq. 2.15. Of course, one needs to keep in mind that this is based on the assumption that the underlying chiral perturbation theory analysis is valid. Currently, we cannot estimate a corresponding systematic uncertainty.

In figure 4 we show  $f_l/f_{PS}$  and  $f_s/f_K$  as functions of  $(r_0 M_{PS})^2$  in the left and right panel, respectively. We have chosen to plot these ratios because it appears that most of the quark mass and lattice spacing dependence cancels. A linear extrapolation of  $f_l/f_{PS}$  in  $(r_0 M_{PS})^2$  to the physical point results in

$$f_l/f_\pi = 0.859(7)_{\text{stat}}(64)_{\text{sys}}. \quad (6.1)$$

However, from the plot it appears that there is still a rather sizeable dependence on the lattice spacing present while the strange quark mass dependence seems to cancel in ratio as all A-ensembles

fall on one single curve. In fact, the systematic error estimated from fitting the data at each value of the lattice spacing separately is one order of magnitude larger than the statistical error and there is clear trend towards larger values of  $f_l/f_{\text{PS}}$  extrapolated to the physical pion mass for decreasing values of the lattice spacing. Therefore, we additionally quote the result of a linear fit restricted to the data at the finest lattice spacing, which yields

$$(f_l/f_\pi)^D = 0.924(22)_{\text{stat}}. \quad (6.2)$$

For the ratio  $f_s/f_K$  most of the strange quark mass dependence is cancelled and the data seem almost perfectly linear in the light quark mass, exhibiting only a moderate slope. Moreover, for this case there are no discernible scaling artefacts within errors and the data are well described by a linear fit which gives

$$f_s/f_K = 1.166(11)_{\text{stat}}(31)_{\text{sys}}, \quad f_s/f_\pi = 1.336(13)_{\text{stat}}(37)_{\text{sys}}, \quad (6.3)$$

at the physical value of the pion mass. Clearly, the systematic error is significantly smaller than the one obtained for the physical value of  $f_l/f_\pi$ , confirming the smallness of any residual lattice artefacts or strange quark mass dependence for  $f_s/f_K$ . The values we obtain are in rough agreement to phenomenological values [24] (and for a very recent one see Ref. [33]), because the spread in the phenomenological estimates is quite large. Still, our estimate for  $f_l/f_\pi$  is a bit lower than expected. We are investigating ways to better control systematics in our analysis.

Finally we have to remark that finite volume effects might play an important role for the decay constants, but they hopefully cancel in the ratios we used.

As discussed in Ref. [33], this determination of mixing parameters can be used to better estimate the hadronic light-by-light contribution to the anomalous magnetic moment of the muon. Of course, eventually a computation of the corresponding transition form factors is desired as recently performed for the neutral pion in Ref. [34].

## 7. Decay Widths $\Gamma_{P \rightarrow \gamma\gamma}$

The decay constants  $f_l$  and  $f_s$  are important low energy constants. However, they can also be used to estimate phenomenologically interesting quantities, most prominently the decay widths of  $\eta, \eta' \rightarrow \gamma\gamma$ . To the same order in the effective theory one can relate the decays widths with the mixing parameters in the quark flavour basis as follows [35, 36] (see Refs. [19, 20] for how to include these quantities into the effective field theory framework)

$$\begin{aligned} \Gamma_{\eta \rightarrow \gamma\gamma} &= \frac{\alpha^2}{288\pi^3} M_\eta^3 \left[ \frac{5}{f_l} \cos \phi - \frac{\sqrt{2}}{f_s} \sin \phi \right]^2, \\ \Gamma_{\eta' \rightarrow \gamma\gamma} &= \frac{\alpha^2}{288\pi^3} M_{\eta'}^3 \left[ \frac{5}{f_l} \sin \phi + \frac{\sqrt{2}}{f_s} \cos \phi \right]^2, \end{aligned} \quad (7.1)$$

where again OZI suppressed terms have been dropped and our normalisation is that  $f_\pi = 130.7$  MeV. Using our lattice data for  $M_{\eta, \eta'}$ ,  $\phi$ ,  $f_l$  and  $f_s$ , we have computed the decay widths and show them in units of the Sommer parameter as a function of  $(r_0 M_{\text{PS}})^2$  in figure 5. We also include the PDG

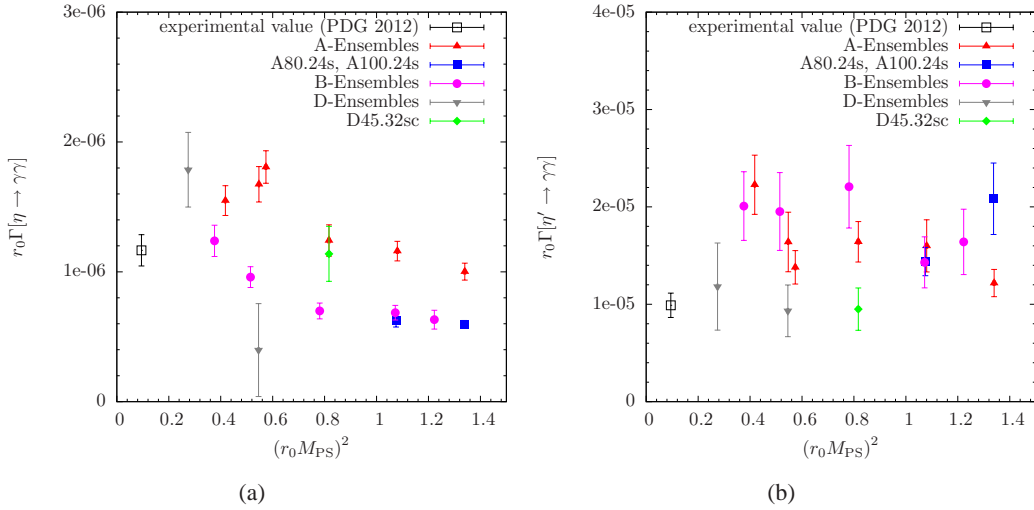


**Figure 5:** We show the decays widths  $\Gamma_{\eta \rightarrow \gamma\gamma}$  (a) and  $\Gamma_{\eta' \rightarrow \gamma\gamma}$  (b) in units of  $r_0$  as functions of  $(r_0 M_{PS})^2$ . In addition we show the corresponding estimate from the PDG [27].

value for convenience [27]. For  $\Gamma_{\eta' \rightarrow \gamma\gamma}$  we observe a flat dependence of the light quark mass and agreement between our data and the PDG value within our errors. However, the data show a tendency for lower values with decreasing values of the lattice spacing.

The situation is not so clear for  $\Gamma_{\eta \rightarrow \gamma\gamma}$ , where the lattice data is of the right magnitude compared to the PDG value. But there are clearly strange quark mass and light quark mass effects visible that we cannot control at the moment. In addition there might be lattice artefacts.

Two remarks are in order: first of all the mass dependence of the widths has not been computed in effective field theory. Hence, we have no rigorous means to extrapolate our data to the physical point. Eqs. 7.1 are strictly speaking only valid in the chiral limit. Second, the PDG value for  $\Gamma_{\eta \rightarrow \gamma\gamma}$  does not include Primakoff experiments, which give a significantly smaller value<sup>1</sup>.

Related quantities are the pseudoscalar transition form factors  $F_{\eta\gamma\gamma^*}$  and  $F_{\eta'\gamma\gamma^*}$  for large momentum transfer  $q^2$ , which can be expressed as [33]

$$\begin{aligned} \lim_{q^2 \rightarrow \infty} q^2 F_{\eta\gamma\gamma^*}(q^2) &= \frac{10}{3\sqrt{2}} f_i \cos \phi - \frac{2}{3} f_s \sin \phi = 96(5)_{\text{stat}}(25)_{\text{sys}} \text{ MeV}, \\ \lim_{q^2 \rightarrow \infty} q^2 F_{\eta'\gamma\gamma^*}(q^2) &= \frac{10}{3\sqrt{2}} f_i \sin \phi + \frac{2}{3} f_s \cos \phi = 274(3)_{\text{stat}}(11)_{\text{sys}} \text{ MeV}. \end{aligned} \tag{7.2}$$

These results have to be understood to be very preliminary. They are obtained by using the values of  $f_i$  and  $f_s$ , Eqs. 6.2 and 6.3, respectively, and the one for  $\phi$  from Eq. 5.1. The systematic uncertainty is again calculated from the maximal difference to results from the separate lattice spacing values.

## 8. Summary

We have presented results for  $\eta$  and  $\eta'$  masses and mixing parameters from lattice QCD with  $2 + 1 + 1$  dynamical quark flavours. The computation is based on gauge configurations provided

<sup>1</sup>We thank P. Masjuan for pointing our attention to this fact.

by the ETM collaboration. Due to an efficient excited state removal method we could determine  $M_\eta$ ,  $M_{\eta'}$  and the mixing angles to good accuracy. For the masses we find excellent agreement with experiment. The mixing angles in the quark flavour basis confirm that  $|\phi_l - \phi_s|/|\phi_l + \phi_s| \ll 1$  and we find the single angle to be close to 46 degrees. This indicates that the  $\eta'$  is dominantly a flavour singlet state.

For the first time we present results for the decay constants  $f_l$  and  $f_s$  using chiral perturbation theory. We find similar values to those found in phenomenology. It is important to keep in mind that  $f_l$  and  $f_s$  are likely to be affected by significant systematic uncertainties due to residual lattice artefacts, quark mass dependence and the approximation in chiral perturbation theory we use.

The extraction of  $f_l$  and  $f_s$  gives us the unique opportunity to estimate the decay widths of  $\eta \rightarrow \gamma\gamma$  and  $\eta' \rightarrow \gamma\gamma$ . Despite the fact that we do not have a rigorous formula for the extrapolation of our data to the physical point we observe ballpark agreement of our data with the current PDG estimate.

We thank all members of ETMC for the most enjoyable collaboration. The computer time for this project was made available to us by the John von Neumann-Institute for Computing (NIC) on the JUDGE and Jugene systems. In particular, we thank U.-G. Meißner for granting us access on JUDGE. We thank P. Masjuan for helpful discussions. This project was funded by the DFG as a project in the SFB/TR 16. K. O. and C. U. were supported by the BCGS of Physics and Astronomie. The open source software packages tmLQCD [37, 38, 39], Lemon [40], and R [41] have been used.

## References

- [1] K. Ottnad, C. Urbach, C. Michael and S. Reker, PoS **LATTICE2011**, 336 (2011), arXiv:1111.3596.
- [2] **ETM** Collaboration, K. Ottnad *et al.*, JHEP **1211**, 048 (2012), arXiv:1206.6719.
- [3] K. Cichy *et al.*, PoS **LATTICE2012**, 151 (2012), arXiv:1211.4497.
- [4] C. Michael, K. Ottnad and C. Urbach, Phys.Rev.Lett **111**, 181602 (2013), arXiv:1310.1207.
- [5] **ETM** Collaboration, R. Baron *et al.*, JHEP **06**, 111 (2010), arXiv:1004.5284.
- [6] R. Baron *et al.*, PoS **LATTICE2010**, 123 (2010), arXiv:1101.0518.
- [7] **ALPHA** Collaboration, R. Frezzotti, P. A. Grassi, S. Sint and P. Weisz, JHEP **08**, 058 (2001), hep-lat/0101001.
- [8] R. Frezzotti and G. C. Rossi, Nucl. Phys. Proc. Suppl. **128**, 193 (2004), hep-lat/0311008.
- [9] R. Frezzotti and G. C. Rossi, JHEP **08**, 007 (2004), hep-lat/0306014.
- [10] **ETM** Collaboration, C. Urbach, PoS **LAT2007**, 022 (2007), arXiv:0710.1517.
- [11] P. Dimopoulos, R. Frezzotti, C. Michael, G. Rossi and C. Urbach, Phys.Rev. **D81**, 034509 (2010), arXiv:0908.0451.
- [12] **ETM** Collaboration, R. Baron *et al.*, JHEP **1008**, 097 (2010), arXiv:0911.5061.
- [13] **ETM** Collaboration, P. Boucaud *et al.*, Comput.Phys.Commun. **179**, 695 (2008), arXiv:0803.0224.

- [14] **ETM** Collaboration, K. Jansen, C. Michael and C. Urbach, *Eur.Phys.J.* **C58**, 261 (2008), [arXiv:0804.3871](#).
- [15] C. Michael and I. Teasdale, *Nucl.Phys.* **B215**, 433 (1983).
- [16] M. Lüscher and U. Wolff, *Nucl.Phys.* **B339**, 222 (1990).
- [17] B. Blossier, M. Della Morte, G. von Hippel, T. Mendes and R. Sommer, *JHEP* **0904**, 094 (2009), [arXiv:0902.1265](#).
- [18] J. Kodaira, *Nucl.Phys.* **B165**, 129 (1980).
- [19] R. Kaiser and H. Leutwyler, [arXiv:hep-ph/9806336](#).
- [20] R. Kaiser and H. Leutwyler, *Eur.Phys.J.* **C17**, 623 (2000), [arXiv:hep-ph/0007101](#).
- [21] J. Schechter, A. Subbaraman and H. Weigel, *Phys.Rev.* **D48**, 339 (1993), [arXiv:hep-ph/9211239](#).
- [22] T. Feldmann, P. Kroll and B. Stech, *Phys.Lett.* **B449**, 339 (1999), [arXiv:hep-ph/9812269](#).
- [23] T. Feldmann, P. Kroll and B. Stech, *Phys.Rev.* **D58**, 114006 (1998), [arXiv:hep-ph/9802409](#).
- [24] T. Feldmann, *Int.J.Mod.Phys.* **A15**, 159 (2000), [arXiv:hep-ph/9907491](#).
- [25] **ETM Collaboration** Collaboration, B. Blossier *et al.*, *PoS LATTICE2011*, 233 (2011), [arXiv:1112.1540](#).
- [26] H. Neff, N. Eicker, T. Lippert, J. W. Negele and K. Schilling, *Phys.Rev.* **D64**, 114509 (2001), [arXiv:hep-lat/0106016](#).
- [27] **Particle Data Group** Collaboration, J. Beringer *et al.*, *Phys.Rev.* **D86**, 010001 (2012).
- [28] **TWQCD/JLQCD** Collaboration, T. Kaneko *et al.*, *PoS LAT2009*, 107 (2009), [arXiv:0910.4648](#).
- [29] N. Christ *et al.*, *Phys.Rev.Lett.* **105**, 241601 (2010), [arXiv:1002.2999](#).
- [30] J. J. Dudek *et al.*, *Phys.Rev.* **D83**, 111502 (2011), [arXiv:1102.4299](#).
- [31] J. J. Dudek, R. G. Edwards, P. Guo and C. E. Thomas, [arXiv:1309.2608](#).
- [32] **UKQCD** Collaboration, E. B. Gregory, A. C. Irving, C. M. Richards and C. McNeile, *Phys.Rev.* **D86**, 014504 (2012), [arXiv:1112.4384](#).
- [33] R. Escribano, P. Masjuan and P. Sanchez-Puertas, [arXiv:1307.2061](#).
- [34] X. Feng *et al.*, *Phys.Rev.Lett.* **109**, 182001 (2012), [arXiv:1206.1375](#).
- [35] T. Feldmann and P. Kroll, *Eur.Phys.J.* **C5**, 327 (1998), [arXiv:hep-ph/9711231](#).
- [36] T. Feldmann and P. Kroll, *Phys.Scripta* **T99**, 13 (2002), [arXiv:hep-ph/0201044](#).
- [37] K. Jansen and C. Urbach, *Comput.Phys.Commun.* **180**, 2717 (2009), [arXiv:0905.3331](#).
- [38] **ETM** Collaboration, C. Urbach *et al.*, *PoS LATTICE2013*, 414 (2013).
- [39] **ETM** Collaboration, B. Kostrzewa *et al.*, *PoS LATTICE2013*, 416 (2013).
- [40] A. Deuzeman, S. Reker and C. Urbach, *Comput.Phys.Commun.* **183**, 1321 (2012), [arXiv:1106.4177](#).
- [41] R Development Core Team, *R: A language and environment for statistical computing*, R Foundation for Statistical Computing, Vienna, Austria, 2005, ISBN 3-900051-07-0.